Research, Society and Development, v. 11, n. 6, e58111629472, 2022
(CC BY 4.0) | ISSN 2525-3409 | DOI: http://dx.doi.org/10.33448/rsd-v11i6.29472

3D printer nozzle modification to obtain scaffolds for use in regenerative medicine

Modificação de bico de impressora 3D para obtenção de suportes para uso em medicina regenerativa

Modificación de una boquilla de impresora 3D para obtener soportes para uso en medicina regenerativa

Received: 04/21/2022 | Reviewed: 04/29/2022 | Accept: 05/07/2022 | Published: 05/12/2022

Franco Henrique Moro
ORCID: https://orcid.org/0000-0003-2442-6316
Institute of Education and Research, Brazil
E-mail: francohm@insper.edu.br
Renata Aquino de Carvalho
ORCID: https://orcid.org/0000-0002-5758-4073
University of Araraquara, Brazil
E-mail: acarvalho@uniara.edu.br
Hernane da Silva Barud
ORCID: https://orcid.org/0000-0001-9081-2413
University of Araraquara, Brazil
E-mail: hsbarud@uniara.edu.br
André Capaldo Amaral
ORCID: https://orcid.org/0000-0001-9625-1442
University of Araraquara, Brazil
E-mail: acamaral@uniara.edu.br
Eraldo Jannone da Silva
ORCID: https://orcid.org/0000-0002-5058-7159
University of São Paulo, Brazil
E-mail: eraldojs@sc.usp.br

Abstract
Use biological or synthetic scaffolds to conduct cellular events of the regenerative process constitute one of the major strategies in regenerative medicine area. Customized scaffolds built by additive manufacturing prove to be a great solution to this problem. Two desired features that aid in scaffold's biocompatibility are the surface roughness and the geometric characteristic of the topography, usually achieved by a chemical procedure performed after printing. This research presented a modification on a 3D printer nozzle for directly generating an external topography in the extruded filaments, eliminating the need for an additional post-processing step. Cell morphology and viability on supports printed by the proposed and conventional method were evaluated in *in vitro* experiments and the new nozzle proved to be efficient in generating printed filaments with a degree of cytocompatibility superior to those obtained by conventional filaments.
Keywords: Hot melt extrusion technology; Tissue scaffolds; Regenerative medicine; Tissue engineering; Printing, three-dimensional.

Resumo
A utilização de suportes biológicos ou sintéticos para a condução de eventos celulares do processo regenerativo constitui uma das principais estratégias na área da medicina regenerativa. Suportes customizados fabricados por manufatura aditiva provam ser uma ótima solução para este problema. Duas características almejadas que auxiliam na biocompatibilidade dos suportes são a rugosidade da superfície e a característica geométrica da sua topografia, geralmente alcançadas por um processamento químico realizado após a impressão. Esta pesquisa apresenta a proposta de obtenção de um bico de impressora 3D capaz de gerar diretamente uma topografia externa nos filamentos extrudados, eliminando a necessidade de uma etapa adicional de pós-processamento. A morfologia e viabilidade celular sobre suportes impressos pelo método proposto e convencional foram avaliadas em experimentos *in vitro* e o novo bocal mostrou-se eficiente em gerar filamentos impressos com grau de citocompatibilidade superior aos obtidos por filamentos convencionais.
Palavras-chave: Tecnologia de extrusão por fusão a quente; Tecidos suporte; Medicina regenerativa; Engenharia tecidual; Impressão tridimensional.

Resumen
El uso de soportes biológicos o sintéticos para conducir eventos celulares del proceso regenerativo es una de las principales estrategias en el campo de la medicina regenerativa. Los soportes personalizados producidos por fabricación aditiva demuestran ser una gran solución a este problema. Dos características deseadas que ayudan en la biocompatibilidad de los soportes son la rugosidad de la superficie y la característica geométrica de su topografía, generalmente logradas por un procesamiento químico realizado después de la impresión. Esta investigación presenta la propuesta para obtener una boquilla de impresora 3D capaz de generar directamente una topografía externa sobre los filamentos extruidos, eliminando la necesidad de un paso adicional de postprocesado. La morfología celular y la viabilidad sobre soportes impresos por el método propuesto y convencional fueron evaluadas en experimentos *in vitro* y la nueva boquilla demostró ser eficiente en la generación de filamentos impresos con un grado de citocompatibilidad superior a los obtenidos por filamentos convencionales.
Palabras clave: Tecnología de extrusión de fusión en caliente; Andamios del tejido; Medicina regenerativa; Ingeniería de tejidos; Impresión tridimensional.

1. Introduction

The replacement of human cells, tissues or organs to restore normal biological functions represents the area of study and application of regenerative medicine (RM) (Mason, & Dunnill, 2008). This area consists of use cell therapy, natural or synthetic biological supports and/or biomolecules, as isolated or associated strategies, to improve the tissue repair process and, consequently, restore more efficiently the biological function after injury or disease (Bartolo et al., 2012). Recently, technologies such as additive manufacturing have been used to create customized biological supports, structures that function as optimized temporary substitutes of the extracellular matrix capable of assisting cell adhesion, proliferation and differentiation and guiding the process of tissue repair (Sampogna et al., 2015; Carvalho et al., 2021). In order, to obtain a good scaffold, it is necessary to use a biocompatible and biodegradable material and that also offers good mechanical resistance to the structure (Machado, 2007). In addition, it is necessary that this scaffold has a porous structure to facilitate the cell migration and tissue ingrowth (Ponciano et al., 2021).

The most used additive manufacturing technology in the world is FDM (Fused Deposition Modeling) (Stratasys, 2018), which can produce printed models with a good porosity control (Hollister, 2005). FDM uses thermoplastic filaments fed by a hot extruder that causes the material to reach its melting point, becoming a viscous fluid, thus allowing it to pass through a nozzle extruder with its outlet hole smaller than the diameter of the filament and therefore, depositing layer by layer in the printing area, where it will return to its solid state, thereby forming the projected 3D object (Designtech, 2018).

The surface roughness and the geometric characteristics of the topography represent relevant factors in the performance of polymeric materials used in the construction of scaffolds, since they can significantly affect the adhesion and cellular differentiation that are fundamental events in the tissue restoration (Liu et al., 2018). Commercial nozzles produce usually extruded polymer with cylindrical section. One of the most used material for scaffolds is the poly (lactic acid) (PLA) (Cheung et al., 2007), this polymer has a good biocompatibility, biodegradability, good processability and a good mechanical resistance (Pawar et al., 2014), PLA implants are rigid and can withstand external stress (Bakhru et al., 1996), therefore, changes in the surface of the scaffold can decrease this resistance. But it generally does not have the ideal surface chemistry and surface topography (roughness and geometry), making necessary the posterior superficial chemical treatment (functionalization) in the printed components (Liu et al., 2018; Chaubey et al., 2008; Abdal-hay, A. et al., 2022) that can lead to a great reduction of its mechanical resistance.

The present research proposes the creation of a nozzle with a new cross-sectional shape, capable of producing macrotexturized (roughness and geometry) filaments that could improve cytocompatibility and try to avoid the use of chemical and physical treatments later in the generated scaffold. Due to its small dimensions the nozzles were manufactured by micromachining. The scaffolds manufactured by this new nozzle were evaluated to verify their influence in the morphology and viability of cells *in vitro*.

2. Materials and Methods

PLA, along with ABS (Acrylonitrile Butadiene Styrene), is the thermoplastic polymer most used by FDM technology (Turner et al., 2014) and is widely used for the manufacture of scaffolds due to the fact that it is biodegradable and biocompatible. It was used in this project the commercial natural filament from Movtech, which has wire diameter 1.75 mm, density of 1.24 g/cm³ and processing condition temperature of 180 ºC – 210 ºC. The commercial nozzle of the brand E3D-online model "Brass V6 Nozzle" with 0.3 mm of diameter, was used in the project to have a good surface quality.

The extrusion nozzle outlet hole has a 0.3 mm cylindrical geometry (Figure 1a). To impose a texture and increase the contact surface of the wire was proposed for that design to apply to the nozzle a geometry as in Figure 1b.

Figure 1. Extruder nozzle outlet holes: (a) prior to wire electro-erosion; (b) after wire electrodes.

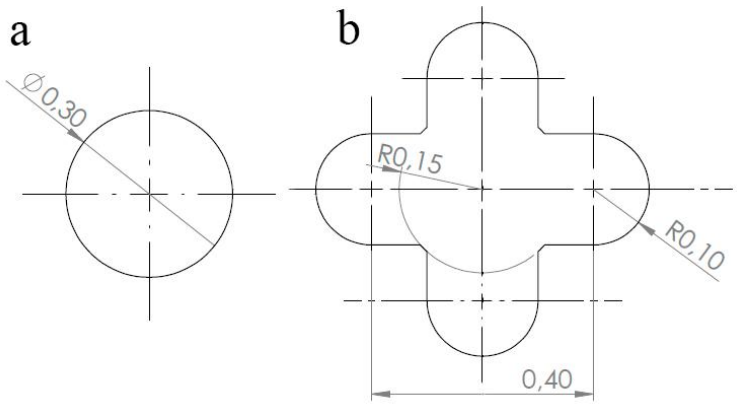

Source: Authors (2018).

A wire-electroforming process was chosen to generate the grooves in the nozzle which is affordable and available in the research region. This process uses precisely controlled sparks between an electrode and a workpiece in the presence of a dielectric fluid (Lucon, 2012). Commercial E3D-Online nozzle was chosen as blanks for the manufacturing process due to its better quality and surface finish. The nozzle was cut using a 0.2 mm diameter molybdenum wire.

Graber i3 model from GTMax3D was the machine used to produce the scaffolds, since it is possible to configure all its parameters and is the most popular model among 3D printing enthusiasts. The extrusion head moves in the X, Y, and Z directions and all movements are controlled by an Arduino board, that reads the G-code and commands the drive. The drive controls the stepper motors.

The geometry of scaffold was selected with 4 total layers with 20 mm diameter with pore size in the 800 μm range, the lower layer being completely filled and the three upper layers consisting of yarns organized in such a way that the yarns of each layer were positioned orthogonally to the wires of the others (Figure 3). In addition, the lateral border is completely filled as well, for a better cellular analysis is possible due to the fact that, with the first layer and the edge completely filled cells, the cell remains inside the scaffold. The fact that, because it has only three porous layers, it is possible to better observe the behavior of the cells in the microscope.

The printer has been configured to produce conventional scaffold with 52 mm/s print speed, curved parts speed of 47 mm/s, internal fill speed of 82 mm/s, printing temperature of 210 °C, table temperature deposition rate of 60 °C, 35% of internal fill and 0.2 mm of layer height. To sanitize the base and to help with the scaffold adhesion, hand sanitizer was used.

For the printing of the textured scaffold, it was necessary to exchange the commercial nozzle by the textured, for that purpose the head was heated to 210 °C, the conventional nozzle was unscrewed and the textured was placed in place. It was necessary to find the best height of the nozzle in relation to the table and began to print the new scaffolds with the same

configurations of the conventional scaffold only differentiating in the height of layer that was used 0.3 mm and the size of the pore was selected around of 500 µm.

Scanning electron microscopy (SEM) was used to visualize the morphology of the scaffolds for evaluation of the surface characteristics of both conventional and textured scaffolds. The scaffolds were coated with carbon and gold for conductivity. These images were then analyzed to measure the fiber diameter and pore size, and to verify the surface modification process. It was also used the Olympus 3D measurement laser confocal microscope model OLS4000 LEXT for visualization of the geometry of the textured nozzle. Simultaneous TG-DSC curves were obtained by a TA Instruments SDT Q600 using nitrogen atmosphere (50 mL min-1) at a heating rate of 20°C min-1 and temperature range of 30 to 600 ºC.

Conventional and textured supports were sterilized with 70% alcohol immersion and subsequent ultraviolet irradiation, and then packed into 12-well cell culture plate. Aliquots of 300 µL of a cell suspension containing 2x105 cells from human fibroblast lineage (GM07492) were gently deposited in the samples from each group (triplicate) and in wells without scaffolds (control). The culture medium used was Dulbecco's modified eagle medium (DMEM-Gibco/Thermofisher), supplemented with fetal bovine serum (SFB10%-Nutricell) antibiotics (Penicillin 10.000U/mL and Streptomycin 10mg/mL-Sigma) and antifungal (Amphotericin B 25ug/mL-Sigma). The wells were photographed for morphological analysis and the plate conditioned in cell culture incubator (PANASONIC) at 37 °C, in humidified atmosphere air (95%) and CO2 (5%) for 24 hours. After 24 hours, the wells were photographed again, the culture medium was removed and the wells were washed with phosphate buffered saline (PBS). Cell viability in the samples was established by the MTT/Formazan colorimetric assay (Mosmann, 1983). Subsequently, 100 µL of MTT (0.5mg/ml) were added to each well and the cells were kept under ideal culture conditions for 4 hours. After this period, 200 µl of isopropanol were added to the wells and gently homogenized for the solubilization of the formazan crystals resulting from the MTT metabolization process. Aliquots of each sample (100 µL) were transferred to 96-well plate and the optical density (OD) values set in spectrophotometer at wavelength (λ) of 570 nm. The OD values were converted into percentages of cell viability in relation to the control group samples (100% of viability) and submitted to statistical analysis (ANOVA ONE-WAY and post hoc Fisher's test) considering a significance level of 5% ($p \leq 0,05$).

3. Results and Discussion

The confocal laser microscope was able to observe the difference between the conventional nozzle with 0.3 mm of diameter (Fig. 2a) and the nozzle hole after passing through the wire EDM process (Fig. 2b).

Figure 2: Images of confocal (a) nozzle with conventional bore exit 0.3 mm; (b) nozzle with textured hole; (c) nozzle with textured hole with the drawing projected.

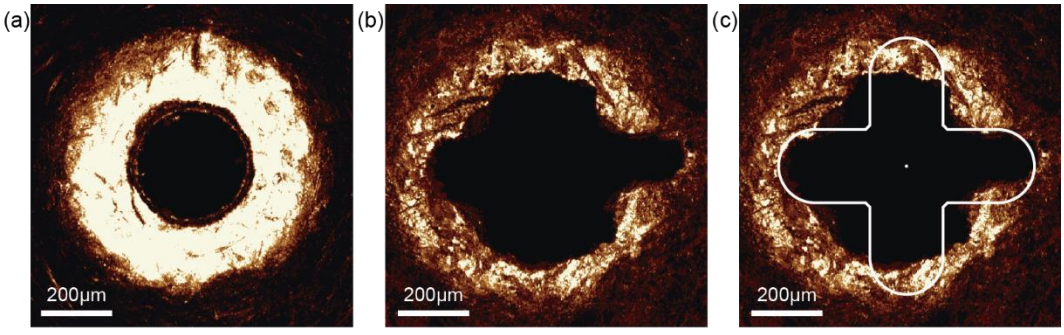

Source: Authors (2018).

As observed in Figure 2c, the planned final geometry was not achieved, this is due to the difficulty of controlling the process that was not accurate, it is also due to the fact that the machining is of micro scale, which makes the grain size large in relation to the tool, as consequence the grain get torn out damaging the hole (Malekian et al., 2012). The electron-beam machining could be used to achieve a greater geometric precision, but because it is a sophisticated process the study would not be replicated to the general public, therefore it was not used. Despite of this issue, the scaffolds manufactured with textured hole showed satisfactory results.

SEM images of the 3D structures are shown in Figure 3. The SEM images of the top and side views clearly show a well-connected structure; it is possible to see clearly the difference in the shape of the wire in Figure 3a and Figure 3b with respect to Figure 3c and Figure 3d; It is also observed in Figure 3d that this shape of the thread remained along every thread.

Figure 3. MEV images of (a) cross-sectional view; (b) and top of the conventional scaffold; (c) cross-sectional view; (d) and top view of the textured scaffold.

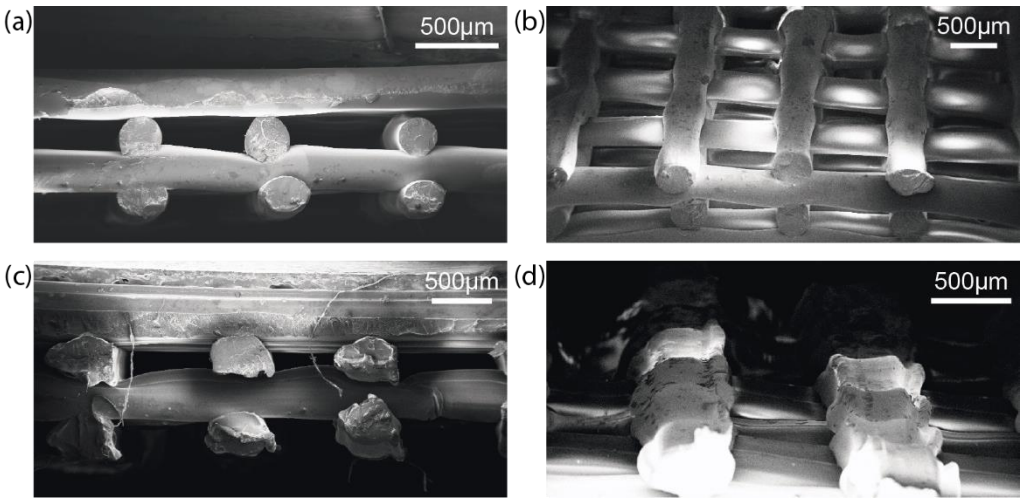

Source: Authors (2018).

A concave shape can be observed in the Fig. 3d which can be an important factor on the cellular differentiation. Although the structure has been programmed to have a uniform pore size of 800x800 µm 500x500 µm, this was not the case in practice. For example, conventional scaffold varied its pore in the range of 725 ± 54 µm and the textured 505 ± 32 µm this variation in pore size probably can be attributed mainly to positioning errors in the drives of the open loop pitch motor. The production of the textured scaffolds presented a great difficulty of production since many took off from the base or had problems in the middle of the impression.

A comparison between surface roughness, conventional and texturized filaments was made by MEV as shown in Figure 4.

Figure 4. Roughness of the wires (a) conventional wire; (b) texturized wire.

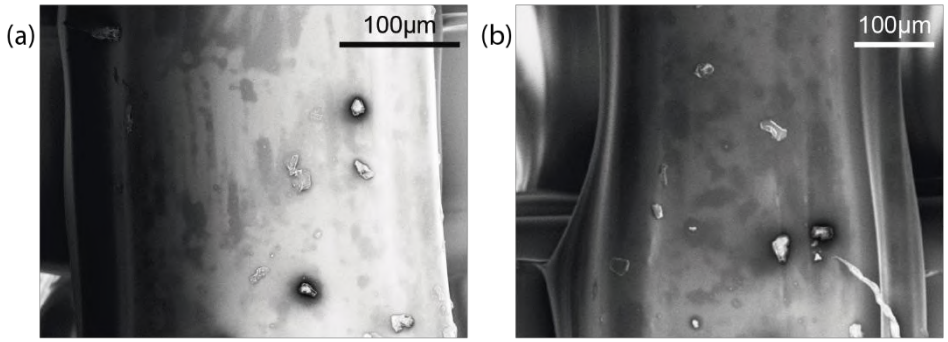

Source: Authors (2018).

Surface modification has an impact in the surface roughness, which is an important factor in biomedical materials, since it can affect cell adhesion (Zhang et al., 2004) the roughness analysis was done in an optical way as in (Liu et al., 2018). Comparing the two images it is possible to notice that there is no apparent difference in surface roughness. Therefore, it is possible to affirm that the cellular viability analysis only took in consideration the geometry of the wire of the scaffold.

The Figure 5 displayed a thermo behavior of all prepared samples using a Simultaneous TG-DSC. TG curves, Figure 5A (a-b) were carryout out in order to verifying the differences in thermal stability for PLA scaffolds samples. Both TG curves for PLA samples display just single-step of thermal decomposition in the range of 240 °C to 390 °C. It can be clearly observed an increase on thermal degradation after the textured nozzle device. This behavior could be associated to increase on the scaffold density due to the new nozzle device.

Figure 5. Simultaneous TG-DSC curves obtained for PLA samples. (A) TG curves for regular PLA samples (a) and texturized PLA sample (b); (B) DSC curves for regular PLA samples (a) and texturized PLA sample (b).

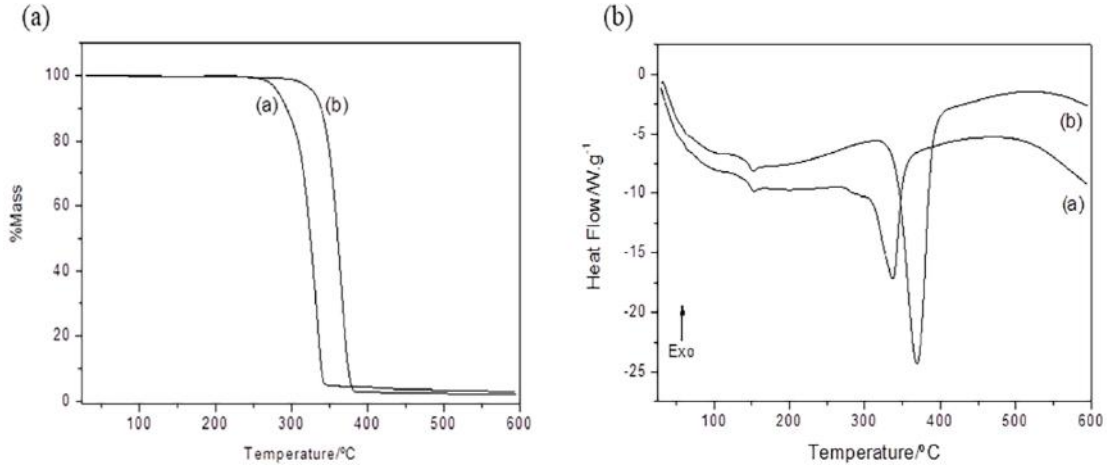

Source: Authors (2018).

DSC curves, Figure 5B (a-b) displayed a change in baseline at around 150 ºC characteristic of the glass transition (Tg) of the prepared PLA scaffolds samples. The endothermic peak between 200 and 300 °C can be related to the thermal decomposition of the PLA. As we observed in the DSC curves, customized PLA sample processed by texturized nozzle device presents an increase on thermal decompositions, and it confirm the same behavior observed on TGA curves.

The results regarding the cell viability assay are presented in Figure 6. There was no difference in viability when comparing the conventional and textured scaffolds and both presented a cell viability lower than the control group. This

difference in relation to the control corresponds to cell preference by adhesion and higher growth rate when exposed to the functionalized polystyrene surface of the culture plate. plate.

Figure 6: Cell viability assay (MTT / formazan) of human fibroblasts (GM07492) seeded in conventional PLA supports, textured PLA and culture plate (Control). Results expressed as percentage of cell viability in relation to the control group (100%). ANOVA ONE-WAY: $P \leq 0.05$. Statistical difference between groups identified by difference in identification letters.

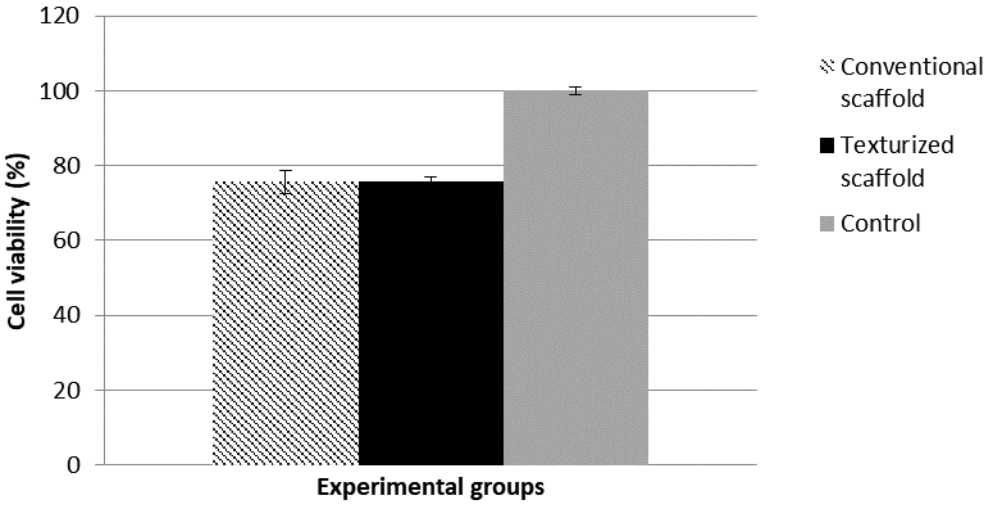

Source: Authors (2018).

Qualitative morphological analysis from light optical microscopy images, performed immediately after seeding the cells on the scaffolds, demonstrated a homogeneous pattern of cell morphology, presenting a typical circular conformation of non adhered cells deposited on the filaments that constitute the coating (Figure 7a and 7c). At 24 hours, the cells seeded in both supports had morphology compatible with the occurrence of adhesion and spreading processes on the surface of the filaments. On the other hand, significant differences in the morphological profile were evidenced when comparing the cells in both scaffolds. The cells in the conventional scaffolds (7b) had a predominantly elongated, non-fusiform morphology with a smaller surface area, suggesting a more restricted interaction (spreading) with the substrate. The cells adhered to the filaments of the textured scaffolds (7d) exhibited a fusiform morphological profile and a larger surface area, suggesting a distinct cytoskeletal organization and a higher degree of interaction with the substrate. These morphological aspects are similar to those of cells normally cultured in culture plates. Similar results were re-ported by Serra and colleagues (Serra et al., 2013) when analyzing the difference in cytocompatibility between PLA and PLA and bio-glass blend (PLA/CaP glass) scaffolds. In this research, mesenchymal stem cells presented a similar patterns in the viability assays and exhibited different morphological profile, with a higher degree of cell/substrate interaction (spreading) in PLA/CaP glass scaffolds. These results were attributed to the topographic and chemical modifications resulting from the blend constitution, responsible for the increase of cytocompatibility. Considering the same chemical constitution of the scaffolds used in this research, the influence on cell/substrate interaction, and consequently on cellular morphology and possibly in cell function, can be exclusively attributed to the topographic changes resulting from the extrusion process by the modified nozzle.

Figure 7: Photomicrography of PLA substrates control ((a) and (b)) and textured ((c) and (d)) immediately after ((a) and (c)) and 24 hours ((b) and (d)) of sowing with human fibroblasts (GM07492). The cells are identified (red circles) as a round format, characteristic of non adhered cells ((a) and (c)), or as a flat fusiform format, characteristic of adhered cells ((b) and (d)), immediately and 24 h after sowing respectively (40x).

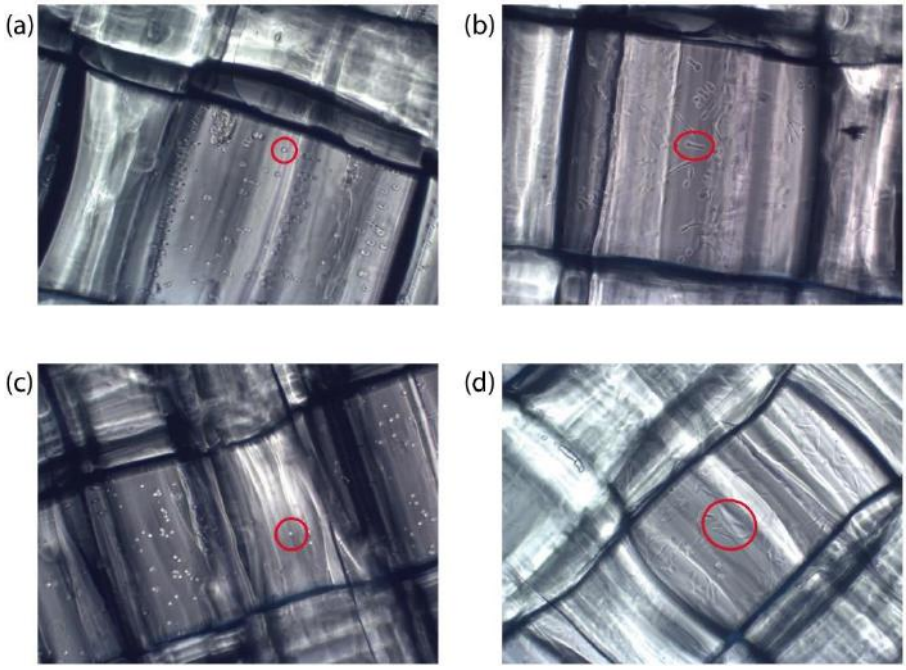

Source: Authors (2018).

The success of a customized 3-D printing biological scaffold for use in regenerative medicine and tissue engineering strongly depends on the topography and chemical properties of the polymer surface after the printing process [18]. Functionalization procedures provided by surface chemical modifications are frequently used to improve the cytocompatibility of scaffolds and to increase their biomodulatory influence on cellular events of adhesion, proliferation and differentiation. In contrast, such modifications may negatively interfere with elementary features such as rate of degradation and mechanical properties of the scaffolds, especially when directed to strategies applied to rigid tissues such as bone. The ability to enhance the cytocompatibility of PLA filaments by the modification of 3D printer nozzle, and consequent direct texturization of the printed filaments in the course of the process, may eliminate the need for additional chemical functionalization procedures, preserving the intrinsic characteristics of the polymer.

4. Conclusion

A new type of nozzle to extrude in FDM was proposed. Analyzes in the microscope were made comparing the conventional filament with the texturized one. The geometry of the filament generated by the proposed nozzle do not improve the cell viability comparing the textured scaffold with scaffolds made with conventional nozzles. The application of this technology for the construction of scaffolds and their use in cell viability is not feasible for improvement in cell growth properties, but the TG and the DSC curves indicated that the texturized scaffold showed an increase on thermal decompositions.

In addition, as a suggestion for future research, it is proposed to perform more tests, using different nozzle geometries and different manufacturing processes that guarantee better control and repeatability.

Acknowledgments

The authors thank the São Paulo Research Foundation (FAPESP, #13/07276-1, and #2018/25512- 8), the National Council for Scientific and Technological Development (CNPq, #407822/2018-6), the ICNT-INFO, the National Foundation for the Development of Private Higher Education (FUNADESP) and TA Instruments Brasil for financially supporting this work.

References

Abdal-hay, A., Sheikh, F. A., Gómez-Cerezo, N., Alneairi, A., Luqman, M., Pant, H. R., & Ivanovski, S. (2022). A review of protein adsorption and bioactivity characteristics of poly ε-caprolactone scaffolds in regenerative medicine. *European Polymer Journal*, *162*, 110892.

Bakhru, H., Bizios, R., Ricci, J. L., & Supronowicz, P. S. (1996). Analysis of osteoblast mineral deposits on three-dimensional, porous, polylactic acid scaffolds. *Trans Annu Meet Soc Biomater Int Biomater Symp*, 2: 848.

Bartolo, P., Kruth, J. P., Silva, J., Levy, G., Malshe, A., Rajurkar, K., ... & Leu, M. (2012). Biomedical production of implants by additive electro-chemical and physical processes. *CIRP annals*, *61*(2), 635-655.

Carvalho, R. A. D., Rocha Junior, V. V., Carvalho, A. J. F., Araújo, H. S. S. D., Iemma, M. R. C., Trovatti, E., & Amaral, A. C. (2021). Poly-(lactic acid) and fibrin bioactive cellularized scaffold for use in bone regenerative medicine: Proof of concept. *Journal of Bioactive and Compatible Polymers*, *36*(3), 171-184.

Chaubey, A., Ross, K. J., Leadbetter, R. M., & Burg, K. J. (2008). Surface patterning: tool to modulate stem cell differentiation in an adipose system. *Journal of Biomedical Materials Research Part B: Applied Biomaterials*, *84*(1), 70-78.

Cheung, H. Y., Lau, K. T., Lu, T. P., & Hui, D. (2007). A critical review on polymer-based bio-engineered materials for scaffold development. *Composites Part B: Engineering*, *38*(3), 291-300.

Designtech. (2018). How Fused Deposition Modeling (FDM) Printers Work. https://www.designtechsys.com/articles/working-fdm-3d-printers.

Hollister, S. J. (2005). Porous scaffold design for tissue engineering. *Nature materials*, *4*(7), 518-524.

Liu, F., Wang, W., Mirihanage, W., Hinduja, S., & Bartolo, P. J. (2018). A plasma-assisted bioextrusion system for tissue engineering. *CIRP Annals*, *67*(1), 229-232.

Lucon, E. (2013). Effect of Electrical Discharge Machining (EDM) on charpy test results from miniaturized steel specimens. *Journal of Testing and Evaluation*, *41*(1), 1-9.

Machado, J. L. M. (2007). Desenvolvimento de Cimento Ósseo de Fosfato de Cálcio como Suporte para Crescimento de Tecidos, 1–161.

Malekian, M., Mostofa, M. G., Park, S. S., & Jun, M. B. G. (2012). Modeling of minimum uncut chip thickness in micro machining of aluminum. *Journal of Materials Processing Technology*, *212*(3), 553-559.

Mason, C., & Dunnill, P. (2012). A brief definition of regenerative medicine. Regen Med [Internet], 3(1):1–5.

Mosmann, T. (1983). Rapid colorimetric assay for cellular growth and survival: application to proliferation and cytotoxicity assays. *Journal of immunological methods*, *65*(1-2), 55-63.

Ponciano, R. C. de O., Costa, A. C. F. de M., Barbosa, R. C., Fook, M. V. L., & Ponciano, J. J. (2021). Scaffolds de quitosana e hidroxiapatita com amoxicilina para reparação óssea. *Research, Society and Development*, *10*(5), e13410514790.

Pawar, R., U Tekale, S., U Shisodia, S., T Totre, J., & J Domb, A. (2014). Biomedical applications of poly (lactic acid). *Recent patents on regenerative medicine*, *4*(1), 40-51.

Sampogna, G., Guraya, S. Y., & Forgione, A. (2015). Regenerative medicine: Historical roots and potential strategies in modern medicine. *Journal of Microscopy and Ultrastructure*, *3*(3), 101-107.

Serra, T., Mateos-Timoneda, M. A., Planell, J. A., & Navarro, M. (2013). 3D printed PLA-based scaffolds: a versatile tool in regenerative medicine. *Organogenesis*, *9*(4), 239-244.

Stratasys. (2018). Tecnologia FDM. http://www.stratasys.com/br/impressoras-3d/technologies/fdm-technology

Turner, N.; Strong, B.R. & Gold, A. S. (2014). A review of melt extrusion additive manufacturing processes: I. Process design and modeling. Rapid Prototyping Journal. 20(3), 192-204.

Zhang, H. X., Du, G. H., & Zhang, J. T. (2004). Assay of mitochondrial functions by resazurin in vitro. *Acta Pharmacologica Sinica*, *25*(3), 385-389.